Electronic transport of bilayer graphene with asymmetry line defects*

Xiao-Ming Zhao(赵小明)[1], Ya-Jie Wu(吴亚杰)[2], Chan Chen(陈婵)[1], Ying Liang(梁颖)[1], and Su-Peng Kou(寇谡鹏)[1,†]

[1] *Department of Physics, Beijing Normal University, Beijing* 100875, *China*
[2] *School of Science, Xi'an Technological University, Xi'an* 710021, *China*

(Received 20 June 2016; revised manuscript received 10 August 2016; published online 30 September 2016)

In this paper, we study the quantum properties of a bilayer graphene with (asymmetry) line defects. The localized states are found around the line defects. Thus, the line defects on one certain layer of the bilayer graphene can lead to an electric transport channel. By adding a bias potential along the direction of the line defects, we calculate the electric conductivity of bilayer graphene with line defects using the Landauer–Büttiker theory, and show that the channel affects the electric conductivity remarkably by comparing the results with those in a perfect bilayer graphene. This one-dimensional line electric channel has the potential to be applied in nanotechnology engineering.

Keywords: bilayer graphene, defects, transportation

PACS: 73.22.Pr, 73.20.Hb, 71.15.Ap **DOI:** 10.1088/1674-1056/25/11/117303

1. Introduction

Recently, graphene, a two-dimensional Dirac material[1–9] becomes an attractive research field due to its exotic quantum properties, such as the unconventional quantum Hall effect, the Klein paradox,[10] the Josephson effect,[11] and the n–p junction.[12] Bilayer graphenes are weakly-coupled two single-layer graphene by interlayer carbon hopping, typically arranged in the Bernal (AB) stacking arrangement. In addition to the interesting underlying physics properties, bilayer graphenes have the potential electronics applications, owing to the possibility of controlling both the carrier density and energy band gap through doping or gating.[13–16] A dual-gated structure allows electrical and independent control of the perpendicular electric field and the carrier density.[17–19] Intrinsic bilayer graphene has no band gap between its conduction and valence bands and the low-energy dispersion is quadratic with massless chiral quasiparticles.[18,20,22] This is in contrast to what is observed in the monolayer which has a linear dispersion with massless quasiparticles.

In this paper, we consider a bilayer graphene with asymmetry line defects and study the defect states and the electric conductivity using the Landauer–Büttiker theory. These nontrivial physics properties of the defect states may be applied to a new type of devices based on the bilayer graphene.

The paper is organized as follows. Firstly, we introduce the tight-binding Hamiltonian of the bilayer graphene. Secondly, we calculate the energy structure of bilayer graphene with line lattice defects. Next, we show the effects of the line defects on the electric conductance, including the effects of defect-line number and the vertical electric field. Finally, conclusions and a summary are provided.

2. The tight-binding Hamiltonian

Bilayer graphene can be classified according to the stacking type. Generally, we focus on AB stacking, with an arrangement that was experimentally verified in epitaxial graphene by Ohta *et al.*[23]

Figure 1(a) is an illustration of a bilayer graphene, that consists of four sublattices A_1, A_2, B_1, and B_2 and the lattice constant is set to unit. To study the system simply, we mainly focus on the non-interaction case, of which an AB-stacked bilayer graphene model only contains first nearest-neighbor (NN) intralayer hopping and NN interlayer hopping. The tight-binding Hamiltonian is given by

$$H_0 = -\gamma_0 \sum_{l,\langle i,j\rangle} \left(a^{\dagger}_{l,i} b_{l,j} + \text{h.c.}\right) - \gamma_1 \sum_i \left(a^{\dagger}_{1,i} b_{2,i} + \text{h.c.}\right). \quad (1)$$

Here, $a_{l,i}$ ($b_{l,i}$) is the annihilation operator at sublattice A_l (B_l) at site $\boldsymbol{R}_i$, where $l = 1$ represents the upper layer and $l = 2$ represents the lower layer of the bilayer material. The first term in the Hamiltonian describes intralayer nearest-neighbor coupling inside the layer, the second term describes the interlayer coupling between the sublattice of the lower layer B_2 and the sublattice of the upper layer A_1 and here we set $\gamma_0 = 3.16$ eV,

*Project supported by the National Basic Research Program of China (Grant Nos. 2011CB921803 and 2012CB921704), the National Natural Science Foundation of China (Grant Nos. 11174035, 11474025, 11504285, and 11404090), the Specialized Research Fund for the Doctoral Program of Higher Education, China, the Fundamental Research Funds for the Central Universities, China, the Scientific Research Program Fund of the Shaanxi Provincial Education Department, China (Grant No. 15JK1363), and the Young Talent Fund of University Association for Science and Technology in Shaanxi Province, China.

†Corresponding author. E-mail: spkou@bnu.edu.cn

© 2016 Chinese Physical Society and IOP Publishing Ltd

$\gamma_1 = 0.39$ eV).[21]

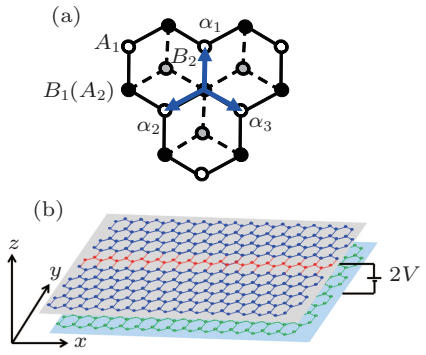


Fig. 1. (color online) (a) The crystal structure of a bilayer graphene with A_1, A_2, B_1, and B_2 sublattices denoted by white, black, black, and gray circles, respectively, 1 and 2 denote the upper layer and lower layers, $\boldsymbol{a}_1$, $\boldsymbol{a}_2$, $\boldsymbol{a}_3$ are primitive lattice vectors. Solid (dashed) lines denote the nearest neighbour links on the upper (lower) layer. (b) Bilayer graphene with line defects on the upper layer marked by red lines. An electric field is applied perpendicular to the layer (z direction) and the corresponding energy difference between two layers is $|2V|$.

Due to spacial translation symmetry, intrinsic bilayer graphene can be described in momentum space and the number of sites in a primitive cell is four. Owing to the inversion symmetry in neutral bilayer graphene, there exists the degeneracy of the highest valence and lowest conduction bands. If the inversion symmetry is broken, a mass gap opens in the low energy spectrum.[24–26] When we assume that the upper and lower layers are at different electrostatic potentials V (normally called bias potentials), the inversion symmetry is broken. Hence, the energy difference between the two layers is parameterized by the energy V. Then, the Hamiltonian becomes

$$\begin{aligned} H &= H_0 + H_{\rm V} \\ &= -\gamma_0 \sum_{l,\langle i,j\rangle} \left(a^{\dagger}_{l,i} b_{l,j} + \text{h.c.}\right) - \gamma_1 \sum_i \left(a^{\dagger}_{1,i} b_{2,i} + \text{h.c.}\right) \\ &\quad + \sum_{l,\langle i,j\rangle} (V_{l,i} a^{\dagger}_{l,i} a_{l,i} + V_{l,j} b^{\dagger}_{l,j} b_{l,j}), \end{aligned} \tag{2}$$

where $H_{\rm V}$ is the external electrostatic potential. Here, we consider a staggered energy potential for bilayer graphene with $V_{1,i} = V$ on the upper layer and $V_{2,i} = -V$ on the lower layer, where $V \geq 0$ is a controllable constant quantity.

3. Localized states induced by line defects

In this paper, we assume that a line-lattice defect lies on the upper layer, as represented by the highlighted red line marked in Fig. 1(b), which is a zigzag lattice chain. To study the line defects on bilayer graphene, we simulate lattice defects on bilayer graphene by the following method: for a target lattice site i on line defects, we set all the coupling hopping parameters connected to the site i to 0 and the local on-site energy potential V_i to be a relatively larger value, i.e., they have essentially been removed from the bilayer graphene. To study the energy spectrum we assume that the bilayer graphene is semi-infinite, that is, the system is finite along the y direction and infinite along the x direction. Thus, the line defect is an infinite zigzag chain along the x direction. To study the localized states induced by line defects, we use the period boundary conditions (PBC) along the y direction which makes the system a nanotube. By performing Fourier analysis and diagonalization, we may obtain the eigenvalues (or energy spectrum) $E(k_x)$ and the corresponding eigenstates. The effects of the line defects and vertical electric potential are shown in Figs. 2, 3, and 4, respectively. For the case of $V > 0$, there exists a bulk energy gap, and the value of the gap becomes larger with the increase of V. In particular, a line defect leads to localized states (or defect states). The electric transport channel from the line defects on one certain layer of the bilayer graphene is not protected by the topological property (for example by the domain wall). Instead, it comes from the broken (generalized) particle–hole symmetry. For the perfect bilayer graphene, the Hamiltonian has the particle–hole symmetry $H = P^{\dagger} H P$, where P is the particle–hole transformation operator for spinless fermion on the honeycomb lattice. We can consider a vacancy as a "hole" in the system by removing a site, it is obvious that such defects break particle–hole symmetry and induce the zero-energy states. The situation is similar to the zero mode induced by vacancy in graphene.

We consider a line defect on the upper layer and set the total number of zigzag chain (parallel to the red zigzag line in Fig. 1(b)) along the y direction to be $N_y = 240$. When $V = 0.00$ there exist defect states (marked by the red solid line and green solid line in Fig. 2(a)) and zero-energy states, which has a flat band. In this case, the wave function of the zero-energy state is localized around the defects (Fig. 2(b)). The length-scale of the localized states along the x direction is $\xi \sim 1/\Delta_{\rm f}$ where $\Delta_{\rm f}$ is the energy gap of the bulk system. In the case of $V > 0$, we also have the localized states around line defects. In this case, a bulk gap appears and the defect states become dispersive. The probability density of zero-energy wave function $|\psi_{E=0}(y)|^2$ becomes extended on both the upper layer and lower layer of the bilayer graphene, and the maximum value of $|\psi_{E=0}(y)|^2$ is on the corresponding positions on the lower layer.

Furthermore, we can also study the cases with several parallel line defects. For two parallel line defects on the upper layer, there exist localized defect states which are located around corresponding line defects, and the electric field induces a finite bulk energy gap (Fig. 4). Because the existence of electrostatic potential can enhance the electron hopping between the lattice in bilayer graphene and weaken the localizing effects of defects, the wavefunction extends.

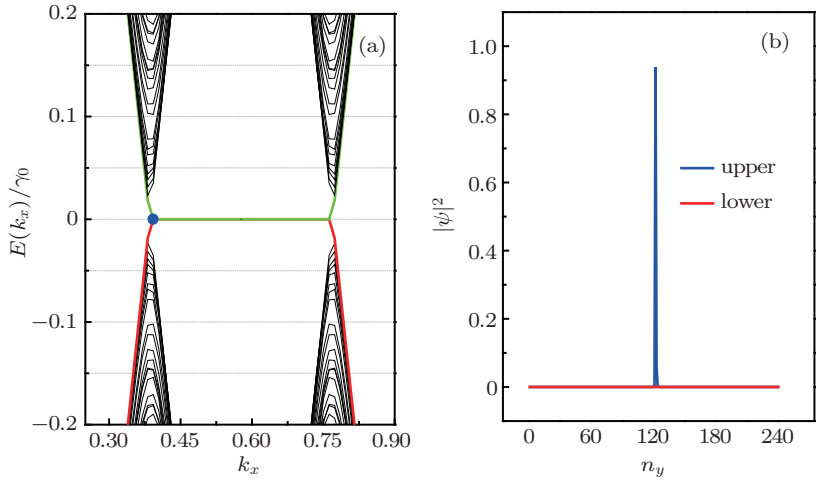


Fig. 2. (color online) Energy spectra and localized states with potential $V/\gamma_0 = 0.00$. The spectra of a single particle in the zigzag bilayer graphene nanoribbons with a line defect located at $n_{y_0} = 120$ on the upper layer is shown in Fig. 1(b), which has PBC along the y direction. (a) Energy spectrum near $E(k_x) = 0$, where the red and green lines denote the defect states of the graphene with a line-defect. The blue dot indicates an energy state with $E(k_x) = 0$. Panel (b) shows the particle-distribution of the zero-energy energy state indicated by the blue dot in panel (a) on the upper layer (blue solid line) and lower layer (red solid line), respectively.

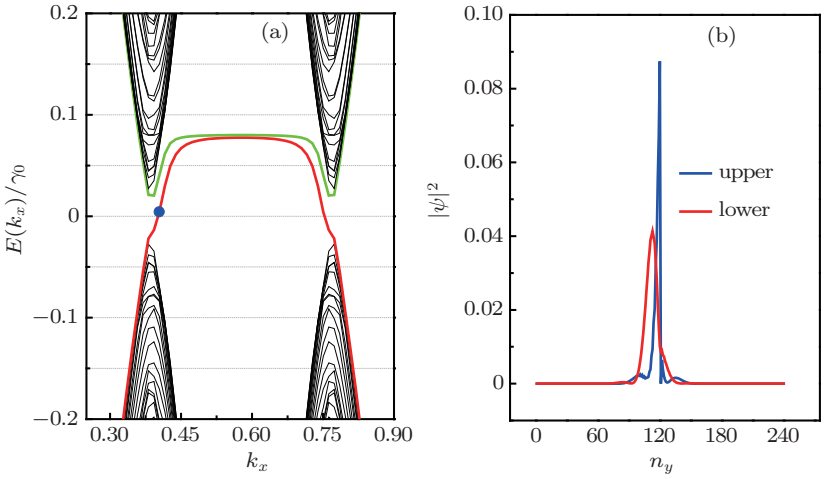


Fig. 3. (color online) Spectra of localized states with potential $V/\gamma_0 = 0.08$. Except for the potential, other conditions are the same as those in Fig. 2. The wave function in panel (b) corresponds to the energy state indicated by the blue dot in panel (a). In this case, an energy gap opens and the dispersion of the defect state has no flat band but looks like an inverted "U".

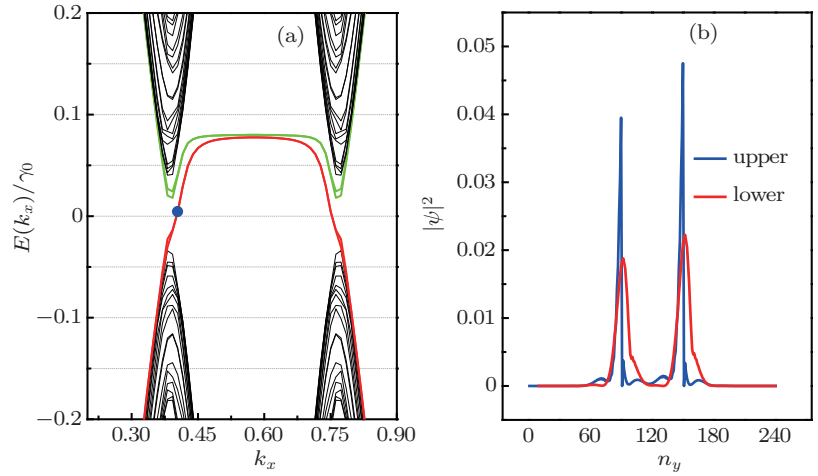


Fig. 4. (color online) Energy spectra and localized states when $V/\gamma_0 = 0.08$. The wave function in panel (b) corresponds to the quantum state of the energy indicated by the blue dot in panel (a). There are two parallel line defects at $n_y = 80$ and $n_y = 160$ on the upper layer.

4. Transport properties of a bilayer graphene with asymmetry line defects

Bilayer graphene exhibits nontrivial transport properties owing to its unusual band structure where the conduction and valence bands touch with quadratic dispersion. One of the earliest theoretical papers studying the conductivity through AB-stacked bilayer graphene is Ref. [27] where it was assumed that the band structure of the bilayer is described by two bands closest to the Dirac point energy. Transport properties and the nature of conductivity near the Dirac point were probed experimentally[1,28] and investigated theoretically.[29]

We use the well-known Landauer–Büttiker equation to obtain the electric conductivity. To show the effect of the line defect on the electric conductance, we separate the original system into three parts: left lead, right lead, and the center device area, as shown in the schematic diagram in Fig. 5. The left and right leads are semi-infinite and the center device area has a finite size. The number of primitive cells along the x direction is N_x; the number of zigzag chains along the y direction is N_y. Here, it is a zigzag edge along the x direction and an armchair edge along the y direction.

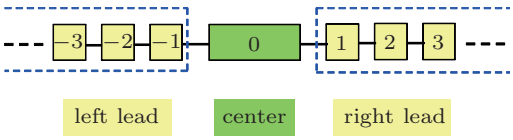


Fig. 5. (color online) The illustration of the system to calculate the electric conductance, which consists of a center device area (denoted by 0 with the green area) and left/right leads (denoted by other integer numbers with the yellow area). The structure of the center can be various, but here we focus on the bilayer graphene with line defects shown in Fig. 1(b).

Hence, for the lead-center-lead bilayer graphene system, the zero-temperature conductance is calculated using the Landauer–Büttiker formalism[30]

$$G = \frac{2e^2}{h}\sum_{\alpha,\beta}(T)_{\beta\alpha}, \tag{3}$$

where $(T)_{\beta\alpha}$ is the transmission from the incoming state α in the left lead to the outgoing state β in the right lead. The terminal electric conductance can be written as $G = (2e^2/h)T$, and the transmission probability T through it is

$$T = \mathrm{Tr}[\boldsymbol{\Gamma}_{\mathrm{L}}\boldsymbol{G}^{\mathrm{r}}_{\mathrm{C}}\boldsymbol{\Gamma}_{\mathrm{R}}\boldsymbol{G}^{\mathrm{a}}_{\mathrm{C}}], \tag{4}$$

where $\boldsymbol{\Gamma}_{\mathrm{L}}$ ($\boldsymbol{\Gamma}_{\mathrm{R}}$) is the left (right) coupling matrix, and $\boldsymbol{G}^{\mathrm{r}}_{\mathrm{C}}$ ($\boldsymbol{G}^{\mathrm{a}}_{\mathrm{C}}$) is the retarded (advanced) Green's function of the center part of the system. The single particle Green's function of the center device area G_{c} is defined as

$$G_{\mathrm{c}} = [(E+\mathrm{i}\eta)\boldsymbol{I} - \boldsymbol{H}_{\mathrm{c}} - \Sigma_{\mathrm{L}} - \Sigma_{\mathrm{R}}]^{-1}, \tag{5}$$

where E is the energy of the particle, η is a positive infinitely-small real number, $\boldsymbol{I}$ represents the identity matrix, $\boldsymbol{H}_{\mathrm{c}}$ is the Hamiltonian of the center device area, and Σ_{L} (Σ_{R}) are the contact self-energies reflecting the effect of coupling of the center part of the graphene to the left (right) leads. We obtain the expressions for the self-energies of the two leads as

$$\begin{aligned}\boldsymbol{\Sigma}_{\mathrm{R}} &= \boldsymbol{H}_{0,1}\boldsymbol{g}^{\mathrm{R}}_{1,1}\boldsymbol{H}_{1,0},\\ \boldsymbol{\Sigma}_{\mathrm{L}} &= \boldsymbol{H}_{0,-1}\boldsymbol{g}^{\mathrm{L}}_{-1,-1}\boldsymbol{H}_{-1,0},\end{aligned} \tag{6}$$

where $\boldsymbol{H}_{0,1}$ ($\boldsymbol{H}_{0,-1}$) is the coupling matrix of the center part to the right (left) lead. Subsequently, we can successfully calculate the electron transmission probability using $\boldsymbol{H}_{1,1}$, $\boldsymbol{H}_{1,2}$, $\boldsymbol{H}_{1,0}$. $\boldsymbol{g}^{\mathrm{R}}_{1,1}$($\boldsymbol{g}^{\mathrm{L}}_{-1,-1}$) are the surface Green's functions of the right (left) leads. Hence, we can determine the conductivity in the presence and absence of line defects.

To compare with the electrical transport effects of the line defects, the electric conductance of perfect bilayer graphene devices is also given (Fig. 6). We use PBC along the y direction, that is, the center device area is a bilayer graphene nanotube. When $V = 0$, the value of G near $E = 0$ is $2(2e^2/h)$, which is double to the value of one layer graphene $2e^2/h$ owing to the degeneracy of the highest valence and lowest conduction bands. When $V > 0$, the value of G at $E = 0$ approaches zero, which indicates that the system generates a bulk energy gap, and the larger V results in a larger width of gap. However, the electric conductance shows additional features induced by the line defects as shown in Fig. 7. When $V = 0$, the value of G near $E = 0$ is about $2e^2/h$. When $V > 0$, there is $G(E) \neq G(-E)$, and from the contrast of pure bilayer graphene and symmetric defects it is clear that this is the result of the particle–hole symmetry breaking by the asymmetric defects.[31,32] Now, the degeneracy of the zero energy is left and the energy spectrum becomes asymmetric. Hence, the conductance can be controlled by the vertical electric potential and the line defects in this case. As a result, this one-dimensional line electric channel has the potential to be applied in nanotechnology engineering.

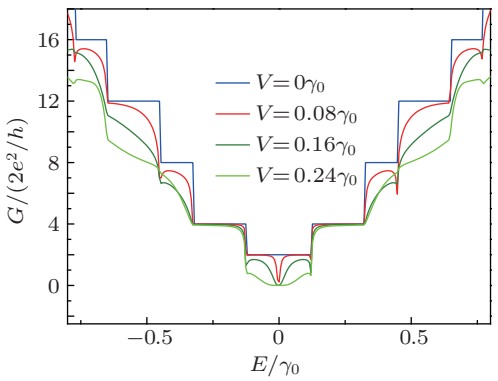


Fig. 6. (color online) The electric conductance with different electric potential V. This is based on a perfect bilayer graphene device with PBC, i.e., bilayer graphene nanotube. When $V/\gamma_0 = 0.00$, the minimum value of G is $2(2e^2/h)$.

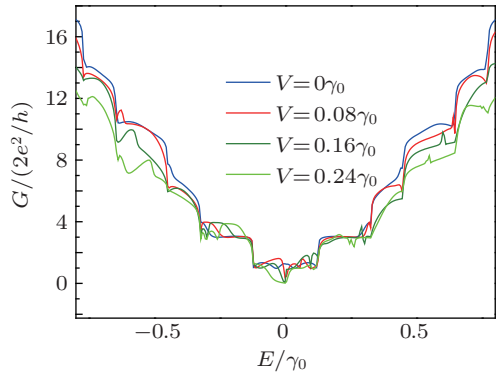


Fig. 7. (color online) The electric conductance with different electric potential V. This is based on a line-defected bilayer graphene device with PBC along the y direction.

5. Conclusion

In this paper, we studied the physics properties of a bilayer graphene with line defects, including the defect-induced localized states and the electric conductivity. We found that the line defect on a certain layer of the bilayer graphene leads to an electric channel. When $V = 0$, the localized states on the single layer have a flat band with zero energy. When $V > 0$, the system becomes gapped and the localized modes have the distribution on both layers. The additional conductance G from line defect is obtained. A first-principle calculation will be done in the further study, it can make the conclusion more powerful and can lead to the defect effects being more practical.This effect from line defects may be applied in electronic devices based on bilayer graphene.

References

[1] Novoselov K S, Geim A K, Morozov S V, Jiang D, Katsnelson M I, Grigorieva I V, Dubonos S V and Firsov A A 2005 *Nature* **438** 197
[2] Zhang Y, Tan Y W, Stormer H L and Kim P 2005 *Nature* **438** 201
[3] Xu X D, Wang Y, Di X and Heinz T F 2014 *Nat. Phys.* **10** 343
[4] Di X, Wang Y and Qian N 2007 *Phys. Rev. Lett.* **99** 236809
[5] Mak K F, McGill K L, Park J and McEuen P L 2014 *Science* **344** 1489
[6] Gorbachev R V, Song J C W, Yu G L, Kretinin A V, Withers F, Cao Y, Mishchenko A, Grigorieva I V, Novoselov K S, Levitov L S and Geim A K 2014 *Science* **346** 448
[7] Novoselov K S, Geim A K, Morozov S V, Jiang D, Zhang Y, Dubonos S V, Grigorieva I V and Firsov A A 2004 *Science* **306** 666
[8] Zhang L C, Shi Z W, Yang R and Huang J 2014 *Chin. Phys. Lett.* **31** 97301
[9] Yan W X 2013 *Chin. Phys. Lett.* **30** 047202
[10] Katsnelson M I, Novoselov K S and Geim A K 2006 *Nat. Phys.* **2** 620
[11] Titov M and Beenakker C W J 2006 *Phys. Rev. B* **74** 041401(R)
[12] Cheianov V V and Fal'ko V I 2006 *Phys. Rev. B* **74** 041403(R)
[13] McCann E and Fal'ko V I 2006 *Phys. Rev. Lett.* **96** 086805
[14] Guinea F, Castro N A H and Peres N M R 2006 *Phys. Rev. B* **73** 245426
[15] Ohta T, Bostwick A, Seyller T, Horn K and Rotenberg E 2006 *Science* **313** 951
[16] Castro E V, Novoselov K S, Morozov S V, Peres N M R, Lopes dos Santos J M B, Nilsson J, Guinea F, Geim A K and Castro N A H 2007 *Phys. Rev. Lett.* **99** 216802
[17] Oostinga J B, Heersche H B, Liu X, Morpurgo A F and Vandersypen L M K 2007 *Nat. Mater.* **7** 151
[18] Zhang Y B, Tang T T, Girit C, Zhao H, Martin M C, Alex Z, Crommie M F, Shen Y R and Wang F 2009 *Nature* **459** 820
[19] Taychatanapat T and Jarillo H P 2010 *Phys. Rev. Lett.* **105** 166601
[20] Sui M Q, Chen G R, Ma L G, Shan W Y, Tian D, Watanabe K, Taniguchi T, Jin X F, Yao W, Xiao D and Zhang Y B 2015 *Nat. Phys.* **11** 1027
[21] Dresselhaus M S and Dresselhaus G 2002 *Adv. Phys.* **51** 1
[22] Shimazaki Y, Yamamoto M, Borzenets I V, Watanabe K, Taniguchi T and Tarucha S 2015 *Nat. Phys.* **11** 1032
[23] Ohta T, Bostwick A, McChesney J L, Seyller T, Horn K and Rotenberg E 2007 *Phys. Rev. Lett.* **98** 206802
[24] McCann E and Falko V I 2006 *Phys. Rev. Lett.* **96** 086805
[25] McCann E 2006 *Phys. Rev. B* **74** 161403(R)
[26] Bostwick A, Ohta T, McChesney J L, Emtsev K V, Seyller T, Horn K and Rotenberg E 2007 *New J. Phys.* **9** 385
[27] Koshino M and Ando T 2006 *Phys. Rev. B* **73** 245403
[28] Zhang Y B, Tan Y W, Stormer H L and Kim P 2005 *Nature* **438** 201
[29] Koshino M and Ando T 2006 *Phys. Rev. B* **73** 245403
[30] Paramita D, Santanu K M and Karmakar S N 2013 *J. Appl. Phys.* **114** 034306
[31] Rhim J W and Moon K 2008 *J. Phys.: Conden. Matter* **20** 365202
[32] Castro E V, Peres N M R, Lopes dos Santos J M B, Castro N A H and Guinea F 2008 *Phys. Rev. Lett.* **100** 026802